

# A prototype telepresence robot for use in the investigation of ebola and lassa virus threatened villages in Nigeria

S.D. Monk<sup>1\*</sup>, E. Jorgensen<sup>1</sup>, A. McCulloch<sup>1</sup>,  
R. Peacock<sup>1</sup>, I. Sangprachatanaruk<sup>1</sup>, J. Azeta<sup>2</sup>, C.A. Bolu<sup>2</sup>, C.J. Taylor<sup>1</sup>

1. Engineering Department, Lancaster University, Lancaster, LA1 4YW, UK  
2. College of Engineering, Covenant University, 10 Idiroko Road, Canaan Land,  
Ota, Ogun State, Nigeria  
s.monk@lancaster.ac.uk

**Abstract:** The article investigates the idea of low-cost, telepresence-based mobile robots for eventual use within villages and rural areas in Nigeria, where diseases such as the Ebola Virus Disease (EVD) and Lassa Haemorrhagic Fever (LHF) are common, yet human intervention is constrained due to the great risk of transmission through bodily fluids. To illustrate the concept and practical issues arising, a systems design approach is taken to identify some of the engineering requirements and, in the focus of this article, a prototype has been developed at Lancaster University. The robotic device is semi-humanoid in that the upper half features two 7-DOF manipulators, designed in part to resemble human operation, while the lower half consists of a four-wheeled base, prioritising ease of operation and reliability over the flexibility offered by a leg-based system.

**Keywords:** Telepresence; First-person viewer; Kinect; Unsafe Environment; Ebola

## 1 Introduction

In 1976, a new filovirus was identified in what is now the Democratic Republic of Congo, which was named the Ebola Virus Disease (EVD) after the Ebola River. A 90% mortality rate was recorded, although this had dropped to around 50% by the time of the 2014 Western African outbreak (which effected Liberia, Sierra Leone, Guinea, Senegal and Nigeria) with improved medical facility development [1-4]. In this breakout, a total of 5481 cases and 2946 deaths were reported, a mortality rate of 54% [5]. Like EVD, Lassa haemorrhagic fever (LHF) is highly transmittable and, therefore, caring for patients with the fever poses a significant risk of transmission. EVD is transmitted through direct contact with body fluids such as sweat, saliva, urine, vomitus, tears, breast milk, stool and respiratory secretions of an infected patient during the severe stage of the disease [6,7]. Some preventive precautions against direct contact include the wearing of protective clothing and the use of standard infection control measures, such as the sterilization of equipment [8]. There is currently no standard treatment for EVD [9-11] outside of supportive care therapies, such as fluid preservation and balancing of electrolytes, oral and intravenous nutritional therapy, maintaining blood pressure and oxygen, and treating other complications that may arise such as secondary infections [4]. It is vital to avoid contact with infected patients, as healthcare related infection was noted as a major cause of transmission in the 2014 outbreak [7]. Techniques to prevent transmission of EVD to health care providers (HCPs) include simple procedures such as putting on and taking off Personal Protective Equipment (PPE) after treatment. This becomes uncomfortable after long periods of use, due to the high temperature and humid conditions, leading to potential human error and reduced effective working hours.

For these reasons, a robotic human stand-in able to perform at least some of the tasks of the people currently required to enter this environment would be greatly beneficial. Human entry time could be significantly reduced if a robotic platform could undertake non-clinical tasks such as the bringing in of general supplies (food and liquids), the removal of rubbish generated (discarded drink cans and food cartons), the cleaning and removal of soiled bedsheets and the removal of human wastes such as urine or faeces. Human-robot interactions have been of interest to the automation community since the 1980's where words like "telerobotics" were first widely used [12] and interactions between humans and robots became more developed [13]. Subsequently, numerous potential applications have been investigated, including rescue robots developed in response to the events of September 11<sup>th</sup> 2001 [14] as well as other disasters and incidents [15]. Despite obvious barriers such as ethical concerns, robotics used in healthcare has also seen a significant volume of work [16]. Prototype mobile robot telepresence systems have included the PRoP [17,18] and the MeBot [19], with off-the-shelf versions now available to the

general public on websites like Amazon. There are also relatively simple telepresence platforms used to stand in for vocations such as tour guides [20], aids for the blind [21] and remote meeting attendance [22]. More complex examples of telepresence robots include Toyota's 32-DOF T-HR3 robot that precisely replicates a seated user's movements using torque sensors [23,24], and the humanoid robot developed by Whitney et al. [25]. Clinical platforms such as the da Vinci robot [26] must obviously be considered here, although the cost is in the region of \$2,000,000 - well out of scope for a medium income country such as Nigeria. Other robots of interest to anyone working in the area of hospital orderly robots may be military robots such as the 'Dragon Runner' and the 'Robo Sally' [27,28], the ChiCaRo (Child Care Robot) [29] used to interact with babies and toddlers and the co-operative robot work by Ilias [30]. Various tele-robotic systems have also been developed to operate in extreme environments that are inhospitable to humans, such as space exploration [31], bomb disposal [32] and nuclear decommissioning [33-35].

This article highlights the motivation and associated research challenge for the use of mobile telepresence robots during EVD and LHF outbreaks. The research aim is to investigate the engineering design requirements, and to build and test in the laboratory a prototype device capable of simple rubbish removal. Standard COTS platforms with two arms and a wheeled base are typically far too expensive to be affordable to the poorly funded and overburdened Nigerian health service. Hence, an important design challenge is to provide a relatively low-cost system for future R&D purposes i.e. the design should be based on off-the-shelf components that have readily available equivalents in the countries effected. The specific objective is to develop a low-cost tele-operated robot that mimics an operator's movements and performs simple operations, such as traversing a flat floor and picking up small and lightweight objects up to a maximum mass of 100 grams. The first prototype will achieve mobility by straightforward wheeled operation.

## 2. Device Concept

Initially, the following requirements have been developed in order to enable the platform to carry out the tasks required:

- Performance optimisation of the proposed device from a technical standpoint must be balanced with a pragmatic realisation that it should be as cheap and as simple as possible, with parts widely available, so that the robot is not only easy to construct anywhere around the world but also straightforward to fix or debug by relatively unskilled labour.
- The device must operable by an unskilled and remotely located person using a Microsoft Kinect V2 based vision system or similar equivalents (available for < £100) to allow robotic mimicry of human movements.
- To optimise the ability of the platform to mimic human abilities, the robot will be of approximately small human height (1.5 m), and feature two arm sized manipulators.
- The platform should be capable of manoeuvring over flat ground at a speed of roughly 3 km/hr (slow to average human walking speed), not exceed a mass of 30 kg, feature two manipulator arms capable of mimicking human movements and sustaining 100 g payloads.
- A First-Person Viewer (FPV) system involving the use of goggles attached to the operator's head will allow remote vision of the environment, with the camera attached to the robot via two servo motors that are used to mimic the operator's movements.

An overarching block diagram of the robotic layout is shown in Figure 1. Here, the operator and robot are linked via Radio Frequency wireless channels with three 14.8 V, 4 cell lithium polymer batteries utilised, one to power the wheels and one used for each manipulator (12 V is used as standard throughout the robot except where this option is unavailable, such as within the microcontroller where 5V is utilised). Low cost and widely available RF XBee modules were selected for the prototype, since they can form a network to increase the range of the system and operate at 2.4GHz, hence reducing interference with the 5.8GHz headset used in the vision system. The XBee-S2S RF transceiver module was chosen due to the small form factor (24 x 27 x 0.5 mm). XBee protocol allows for point to multi-point configurations for networking purposes, with multiple channels to support multiple networks. They are also suitable for long distance applications, using a network of modules as beacons to reach the desired location. Another concern within the scope of this robot design is safety. There are no formally agreed

and published guidelines regarding Nigerian robot safety standards, although there is a small volume of work published regarding robot safety generally e.g. [36,37]. Most industrial safety standards [38] focus on isolating the robot from humans, something that will be implemented here implicitly. The use of PAN IDs and addresses within the Xbee RF communication protocol used here, allows the user to effectively lock the module to prevent data being received from other devices.

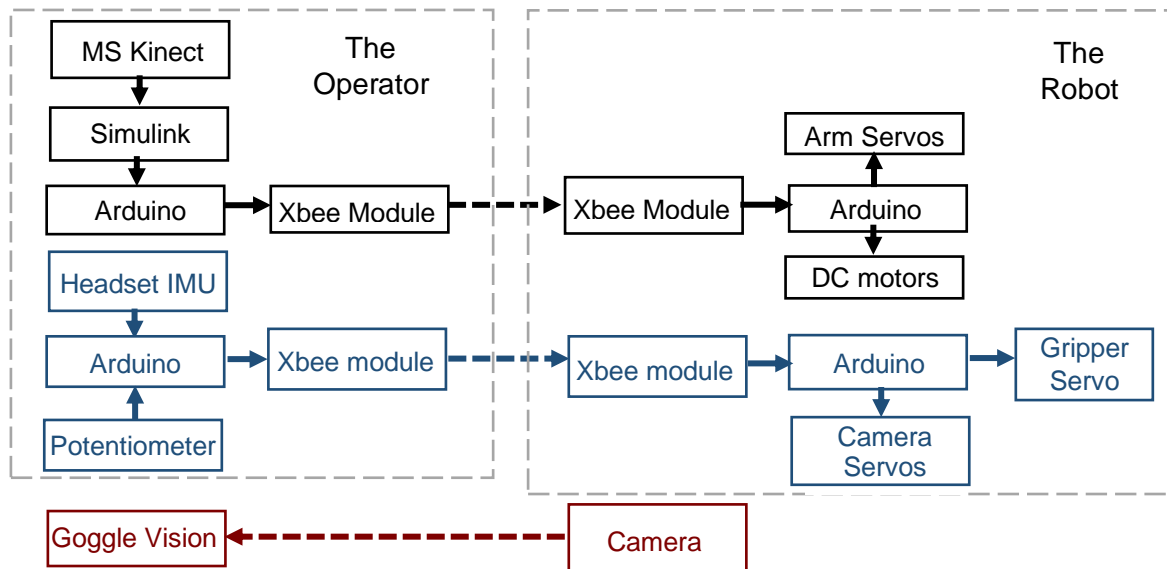


**Figure 1:** Block diagram of the prototype showing the communication pathways.

### 3. Mechanical Design

Considering the need for reliability within a remote location, a four-wheel based design was employed for the prototype. The construction can be summarised into three parts: the wheelbase, the spine and the arms. The wheel base and spine are designed in a straightforward manner with four, 15 cm diameter wheels attached to 5 Watt brushed DC motors with a 50:1 gearbox attached, each one thus producing a stall torque of 4.12 N.m at 100 RPM, corresponding to a maximum speed of 2.83 km hr<sup>-1</sup>. The base has a width of 50 cm, a depth of 35 cm and a height of 15 cm. The spine is constructed in a similar way with a height of 150 cm as illustrated in Figure 2(a). Finite Element Analysis (FEA) was used to evaluate extreme load case performance, with the results indicating that either aluminium or steel would both be durable enough for this application since very high concentrations of stress are unlikely. In fact, 1050A grade aluminium with a yield strength of 90 MPa and ultimate tensile strength of 120 MPa was chosen for the prototype.



**Figure 2 (a)** The wheels base and robot body.



**Figure 2(b)** Arms and shoulder system.

The manipulator arms comprise in-joint actuation and simple metal limbs to connect the joints, with an acrylic end effector designed to pick up objects, such as empty drinks cans or bottles. The arms are designed with brackets

and 1050A aluminium metal, together with custom machined and additive manufactured components. The joints are actuated by Dynamixel servo motors to achieve an 8-Degree of Freedom (DOF) arm overall (3-DOF in the shoulder, 2-DOF in the elbow and 3-DOF in the wrist and hand) as shown in Figure 2(b). Each arm uses one 7.3 N.m torque dynamixel MX-64 motor in the shoulder, with three 3.1 N.m MX-28 motors and three 1.5 N.m AX-12 motors used through the rest of the arm, except for the gripper itself which is actuated with a 1.1 N.m towerpro mg995 motor. Servos such as the Dynamixels offer high-resolution performance with daisy-chain connections, enabling easier logistical control. The prototype is thus comparatively easy to create and maintain although an alternative is to utilise lower-cost DC motors, albeit requiring a more complex arm design than the present prototype, featuring embellishments such as gearing. The main performance criteria of the constituent parts within the arm is that the stall torque can maintain any requested joint angle at maximum load conditions. In this regard, Figure 3 illustrates the manipulator arms in the horizontal configuration, where the maximum load will be experienced by three of the motors A2, A4 and A6. MX represents the mass of the payload utilised, while lengths L1 to L5 are the links between the centre of masses M1 to MX, all shown in Table 2. Subsequent torque calculations are shown in Table 3. The motors all possess enough torque to successfully perform the operations required, although motor A2 is clearly the limiting node, as this may be run at 90% of capacity when a load of 100 g is used.

**Table 2:** Mass and length of each manipulator component.

Object	Mass (g)	Length (mm)
M1	188	-
L1	52	75
M2	188	-
L2	17	246
M3	156	-
L3	15	181
M4	132	-
L4	0	30
M5	159	-
L5	0	90
MX	100	-

**Table 3:** Maximum and available torque for each manipulator motor.

Motor	Maximum N m	Available N m	Capacity %
A1	2.78	7.3	38
A2	2.78	3.1	90
A3	1.08	3.1	35
A4	1.08	3.1	35
A5	0.38	1.5	25
A6	0.38	1.5	25

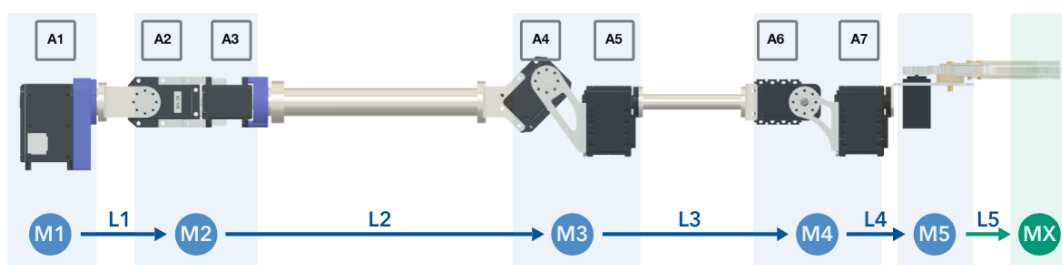


**Figure 3:** The motors in each manipulator at maximum load configuration.

## 4. Motor Control

Entry level Arduino microcontroller boards such as the “Mega” and “Nano” (featuring ATmega2560 and ATmega328 microcontrollers respectively) are selected for the prototype because of their relatively low price and wide availability in Nigeria. Periodically, data sent from the Kinect are not received in the order anticipated, causing significant problems in the development of the robot control system. Hence, a data encryption technique was introduced to the code, in which a number ID was assigned to each segment of data sent. A Kinect V2 sensor (depth range 0.8 m to 4.0 m, a vertical angle limit of  $43.5^\circ$  and a horizontal angle limit of  $57^\circ$ ) was selected for the prototype. The sensor allocates 25 joints per person, as illustrated by Figure 4, with C# used to manipulate the output together with OpenNI APIs – an open source package for 3D sensing utilising middleware libraries. The Simulink toolbox ‘Simulink Real-Time’ was used with metadata obtained using a ‘From Video Device’ block. The metadata includes ‘JointPositions’; a  $25 \times 3 \times 6$  matrix indicating the location of the 25 joints of a tracked body in 3-D space. This contains firstly the joint number, secondly the X, Y and Z coordinates of the positions of the joints relative to the Kinect in meters, and thirdly; code to represent which of the six bodies is being considered.

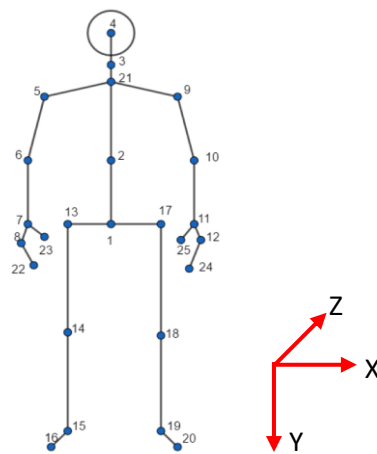


**Figure 4:** The points of the human body as utilised by the Kinect.

The origin is shifted 0.75 m downward and to the left. Angle data calculated within the Simulink environment is transmitted for actuation of the Servo motors [39] via the microcontrollers and RF modules. Due to limitations in the spatial resolution of the Kinect device, hand tracking became unreliable and so control of the end-effectors was subsequently transferred to linear potentiometers held in the operator's hands, with the collected data sent along with the head pitch and yaw data using the 5.8GHz signal channel. The shoulder and elbow of the robot are illustrated in Figures 5(a) and 5(b) respectively, with the gripper mechanism shown in Figure 5(c). Human shoulders, elbows and wrists feature far greater flexibility than is currently mechanically realisable and, therefore, two servo motors are used to represent each of the shoulder and elbow joints.

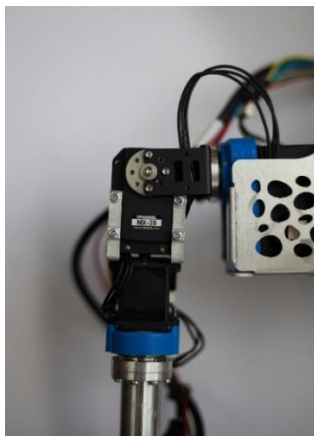


**Figure 5(a)** Robot shoulder joint.



**Figure 5(b):** Robot elbow joint.



**Figure 5(c):** The gripper

Motor A1 is in the shoulder of the robot and controls the degree to which the manipulator arm swings forward and back i.e. the Y and Z orientation. The angle associated with motor A1 ( $\theta_{A1}$ ) is calculated in a two-dimensional perspective using straightforward trigonometry as illustrated in equations (1) and (2).

$$V_{upper} = \begin{bmatrix} a \\ b \\ c \end{bmatrix} = \begin{bmatrix} J10_x - J9_x \\ J10_y - J9_y \\ J10_z - J9_z \end{bmatrix} \quad (1)$$

$$\theta_{A1} = \tan^{-1} \left( \frac{c}{b} \right) \quad (2)$$

where  $V_{upper}$  represents the vector of the upper arm, with  $a$ ,  $b$  and  $c$  defined as components of the vector between joints J9 (the shoulder) and J10 (the elbow) as illustrated in equation (1). Here,  $J10_y$  for example represents the Y component of point J10 in Figure 6(a).

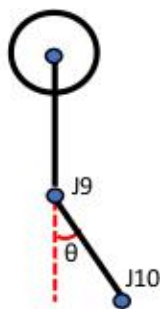


**Figure 6(a)** Manipulator movement (Motor A1)

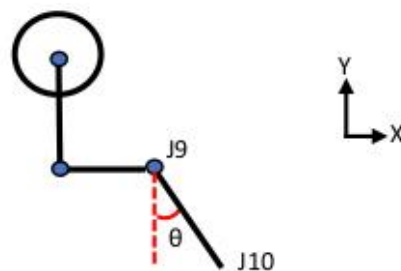


**Figure 6(b)** Manipulator movement (Motor A2)

Motor A2 causes movement of the upper arm away from the body i.e. nominally in the X and Y planes, as shown by Figure 6(b). Hence, a similar calculation as for equations (1) and (2) can be used. The angle  $\theta_{A2}$  is determined in equation (3).

$$\theta_{A2} = \tan^{-1} \left( \frac{a}{b} \right) \quad (3)$$

The actuation of motor A3 represents the upper arm rotation. Since there are no restrictions on the movement, a reference axis is required to determine the angle of rotation. The angle is calculated from the reference axis to the vector from point J9 (the shoulder) to J10 (the elbow). However, in a three-dimensional system, there are an infinite number of perpendicular lines that can be found with such a vector, hence some arbitrary values are set to fix a solution. Here, the vector of the upper arm (1), is considered as an input vector obtained directly from the Kinect sensor with the reference vector which is orthogonal to the upper arm  $V_{perp}$  in Equation (4). Similar to the upper arm vector in equation (1),  $V_{lower}$  is defined as the vector between the elbow (J10) and wrist (J11) as defined in equation (5).

$$V_{perp} = \begin{bmatrix} u \\ v \\ w \end{bmatrix} = \begin{bmatrix} 1 \\ 0 \\ -\frac{a}{c} \end{bmatrix} \quad (4)$$

$$V_{lower} = \begin{bmatrix} p \\ q \\ r \end{bmatrix} = \begin{bmatrix} J11_x - J10_x \\ J11_y - J10_y \\ J11_z - J10_z \end{bmatrix} \quad (5)$$

At this juncture, two assumptions are made, firstly that the elbow of the operator will always go forward of the body rather than backwards (i.e.  $c$  will always be positive), and secondly that  $a$ ,  $b$  and  $c$  will all be non-zero. This realistic constraint simplifies the calculation of the perpendicular reference vector. Once the reference axis has been determined, the rotation angle between the lower arm and the reference axis is determined as in equation (6), while ignoring the Y-component, since the rotation will be relative to a vertical and reference axis,

$$\theta_{A3} = \cos^{-1} \left( \frac{p * u + r * w}{\sqrt{p^2 + r^2} * \sqrt{u^2 + w^2}} \right) \quad (6)$$

The angle of motor A4 is determined in a similar manner, except that here the relevant vector is considered between the upper and lower arm components as defined in equation (7)

$$\theta_{A4} = \cos^{-1} \left( \frac{p * a + r * c}{\sqrt{p^2 + r^2} * \sqrt{a^2 + c^2}} \right) \quad (7)$$

Motor A8 determines the degree of grip and is directly altered using a linear potentiometer in the hand of the operator, as noted above. Motor A7 determines the roll of the hand and uses feedback from the IMU on the operator's hand to ensure the manipulator hand is always parallel to ground. Similarly, motor A6 manages the pitch of the gripper and uses another axis from the gyroscope to calculate this requirement. Finally, motor A5 controls the rotation of the lower arm and achieves this by assuming the gripper/hand will always be required to face forwards i.e. parallel to the Z-axis. Hence, data from the IMU will allow consistent updating of this information to ensure the gripper stays in the required orientation. Due to noise in the Kinect data, the measured positions generally fluctuate by a small amount, leading to noticeable fluctuations in the calculated angle of between 1° to 4°. To address this issue, a filter based on comparing the current angle with the previously sampled angle was designed. Finally, the driving system of the robot uses a signal measured from movement of the operator's feet. The movement is registered by the Kinect and converted to a value that dictates how the robot moves. There are two signals for the driving system, namely a driving signal (forward/backward) and a rotating signal (left/right). The position of each foot was measured with the spine base as a reference point.

## 5. Operator Vision

A 2-DOF system was developed for this robotic prototype, with pitch and yaw being controlled independently and roll not implemented. This action simplifies the mounting design and allows for more stable code development. A Fatshark 600TVL CMOS camera was utilised with the corresponding Fatshark Predator V2 goggles providing a feeling of immersion in the environment to the user. In order to determine the operator's head orientation, an MPU6050 three-axis accelerometer and gyroscope is used. Two RF data streams are thus operational between the user goggles and the robot camera: transmission of the visual image from the camera to the goggles; and the orientation of the goggles which is transmitted towards the servo motors that subsequently determine the orientation of the camera. The 3D printed camera mount design consists of four parts: a base plate, two sections for the main body and one part to hold the camera and pitch servo, as shown in Figure 7(a). The Fatshark goggles as shown in Figure 7(b) are employed as the mounting point for the MPU6050, the microcontroller and XBee module used for RF transmission, with the MPU6050 Jarzebski library used to determine the IMU data. A threshold value was established via preliminary experimentation, and programmed into the software, to allow the user to specify the level of movement required to register as head movement as opposed to noise. A filter was developed to combine the accurate, but less stable, gyroscope data with the less accurate, but rather more stable accelerometer data. Another problem encountered was that the value returned by the gyroscope can drift from the actual value due to the gyroscope being integral. The position is thus only known relative to its previous position with the integral of the error causing the drift. This was partially rectified by the design of another filter, which reduces the drift to a rate of 1° per minute. Further improvements are realised by altering the threshold value, such that very small movements were ignored by the system completely.



**Figure 7(a)** The CMOS camera and servo

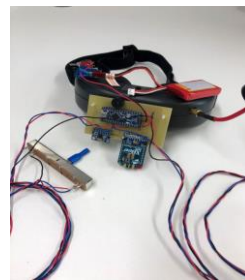


**Figure 7(b)** Goggles, IMU, Nano, Xbee RF

## 6. Testing

Initial testing of the robot was undertaken in order to determine whether the device traverses the floor when the operators foot is lifted from the floor and orientated either (i) straight ahead to indicate that both motors should drive forward or (ii) to one side to indicate that one of the sets of motors (left or right) should operate and thus the robot will orientate accordingly. These tests confirm that the Kinect can detect movement in the operator and the software algorithm implemented translates this into robotic actuation at a rate of around  $2.4 \text{ km.hr}^{-1}$ .

The second part of the test involved the lifting up of a drinks bottle containing 100 ml of liquid. The Kinect is successfully able to identify movement in the individual constituents of the operators arm (shoulder, elbow and wrist) and translate this into movement. The information transmitted from the MPU6050 allowed the hand of the robot to operate smoothly, providing operator movement is kept quite languid and with no sudden acceleration. The combination of these data streams from the Kinect and the IMU allowed the end effector to be positioned around the plastic bottle. The linear potentiometer held by the operator allowed gripping motion to occur and thus the object was grasped and subsequently lifted successfully.

Inaccuracies in the exact position of the end-effector are sometimes observed which are ascribed as due to two major factors. Firstly, deviations in dimensions between the arms of the operator and the arms of the robot, and secondly an angular offset in the servo motors. Furthermore, due to latency within the system, the end-effector occasionally displays a jolting motion, impacting on its ability to perform precise movements. Although this is not an issue with a durable object such as a drinks bottle, it may be a hindrance if more precise movements are required in a future iteration of the device. This latency is likely caused by several small contributions from various elements in the system, such as the Kinect, the signal processing, sending data and IDs, receiving data, assigning data and writing the data to the specific motors. Slight jolting motion is generated as the different angles are assigned causing the motors to move to the next point and stop repetitively. To diminish this, the rate of the motors is reduced as much as possible to create smoother motion. Finally, once the operator has placed the end effector/gripper around the object, visual feedback from the camera is successfully used to determine the grip required through a simple trial and error method.

## 7. Discussion

The prototype device built and tested in Lancaster has proven to be fit for basic tasks within a laboratory environment. In future work, the device will be recreated on site at Covenant University in Nigeria in order to mimic 'real life' scenarios. The present work has concentrated on determining a compromise between utilisation of parts that are most suitable for the task (from a performance and engineering design perspective) and parts which are readily available worldwide, as well as being cheap enough for easy replacement and simple enough for future use and alteration by non-experts. Whilst the robot reported in this article is useable within laboratory conditions, a device for use *in-situ* for realistic conditions in Nigeria will require several improvements.

Torque within the Dynamixel MX-28 motors used in the robot manipulator arms was a constant problem, with servo motors operating near to their limits, a situation that could lead to their required replacement over time. As noted above, the MX-28 motor used in the shoulder experiences the greatest torque demand to availability ratio, although any of these motors could become damaged and thus could require replacement at any time. Unfortunately, the Dynamixel motors are relatively expensive (~£200 each) and are not generally found locally in Nigeria. These servo motors were chosen for the prototype because of their relatively high torque and ease and precision of control. Use of simpler and more common DC motors will necessitate a redesign of the arms, a stage that is likely to require some gearing. Furthermore, the current wheel base is only suitable for relatively flat areas, whereas the addition of embellishments such as larger pneumatic wheels or an active suspension system might allow movement over less structured terrains.

There is also scope for implementation of a haptic feedback system in the robot gripper to enable suitable grip strength at all times. Currently, the only aspect of the robot that could be described as semi-autonomous is the gripper, since it features a 3D gyroscope on top of it ensuring that the end effector stays parallel to earth. However, a force feedback system would enable further implementation of semi-autonomous control. The robot will also need to be ruggedized, so that it can survive harsh conditions when used. The device is currently operational only

in lab conditions and over relatively short periods of time. Repairs are likely to be difficult within field conditions and thus close to 100% reliability will be essential. Also essential is a system of wireless communication which can be operational wherever required. Basic RF communications modules were used in the present research for convenience, but this may not be suitable in field conditions and over significant distances.

Depth perception is not enabled here and is not something that would be an obvious necessity for implementation as 3D vision systems involving two cameras are widely available although this leads to greater complications within the coding requirement as well as possible increases in latency. The simplicity of the robot in its current state means that using simple proportional control is adequate. However, it is anticipated that future iterations of the device would further evolve in terms of the control system utilised. Another consideration to consider in future work may be in the societal and financial effect such a device may have, if ever fully incorporated into Nigerian contagious disease wards. Potential loss of employment for local people as well as simple mistrust of technology in some cultures, may provide a greater barrier than expected.

Finally, significantly tougher testing is required both in the laboratory and in real-life conditions. A possible testing methodology may be the NASA task load index (NASA TLX) assessment which requires users to subjectively rate a task on six different areas. Groups such as Marturi et al.[40], have used the human factors approach while investigating the effect of adding a level of autonomy to direct tele-operation systems. The index features questionnaires answered by the participants who subjectively rate the workload on 6 different sub-scales: mental demand, physical demand, temporal demand, effort, frustration level and overall performance.

## 8. Conclusions

A tele operational robot prototype for supporting health care providers during outbreaks of Ebola and Lassa virus disease has been designed and built. It can successfully mimic an operator's movements and perform simple operations such as traversing a flat floor and picking up small and light objects, up to a maximum mass of 100 grams. The robot designed at Lancaster University and reported in this article will be recreated with the partner university in Nigeria for further testing, initially in the context of an indoor environment. However, a number of changes and implementations are required in the design of the robot before it can be utilised *in situ* for the intended long-term application, namely investigations of disease threatened villages. The upgrades most needed are in the ruggedization of the device to facilitate its operation in real-life conditions at high levels of reliability. All these issues need addressing whilst also considering cost and other local practical constraints, and these are the subject of on-going research by the authors.

## Acknowledgements

This work is, in part, supported in the UK by the EPSRC project EP/R02572X/1.

## References

1. World Health Organization Ebola Response Roadmap Situation Reports, <http://www.who.int/csr/disease/ebola/situation-reports/archive/en>. Last accessed on 26/05/2020.
2. Sanchez, A., Geisbert, T.W. & Feldmann H.: Filoviridae: Marburg and Ebola viruses. Fields Virology.; 5th Edn. Philadelphia: Lippincott Williams & Wilkins, pp. 1409–48 (2007)
3. Report of an International Commission, Ebola haemorrhagic fever in Zaire, Bulletin of the World Health Organization, 56 (2), 271-293 (1976)
4. Tseng, C.P., Chan, Y.J.: Overview of Ebola virus disease. Journal of the Chinese Medical Association 78 (1), 51-55 (2015)
5. Alexander, K.A., Sanderson, C.E., Marathe, M., Lewis, B.L., Rivers, C.M., Shaman, J., Drake, J.M., Lofgren, E., Dato, V.M., Eisenberg, M.C. & Eubank, S.: What Factors Might Have Led to the Emergence of Ebola in West Africa?. PLOS Neglected Tropical Diseases 9(6) (2015)
6. Fauci, A.S.: Ebola-underscoring the global disparities in health care resources. N. Engl. J. Med. 371 (12), 1084-6 (2014)
7. Moghadam, S.R.J., Omid, N., Bayrami, S., Moghadam, S. J. & Seyed Alinaghi., S.: Ebola viral disease: a review literature. Asian Pacific Journal of Tropical Biomedicine 5 (4), 260-267 (2015)
8. Ogbu, O., Ajuluchukwu, E. & Uneke, C.J.: Lassa fever in West African sub-region: an overview. Journal of vector borne diseases 44 (1), 1 (2007)
9. World Health Organization, Ebola Virus Disease factsheet, <http://www.who.int/news-room/fact-sheets/detail/ebola-virus-disease>. Last accessed on 26/05/2020

10. Althaus, C.L., Low, N., Musa, E.O., Shuaib, F. & Gsteiger, S.: Ebola virus disease outbreak in Nigeria: transmission dynamics and rapid control. *Epidemics* **11**, 80-84 (2015)
11. Weyer, J., Grobelaar, A. & Blumberg, L.: Ebola virus disease: history, epidemiology and outbreaks. *Current infectious disease reports* **17** (5), 21 (2015)
12. Sheridan, T.: Human supervisory control of robot systems. *Proceedings. IEEE International Conference on Robotics and Automation* (Vol. 3, pp. 808-812). IEEE (1986)
13. Harless, M., Donath, M.: An intelligent safety system for unstructured human/robot interaction. *Proceedings of the Robots Conference and Exposition*. 117-120 (1985)
14. Murphy, R.R.: Rescue robotics for homeland security. *Communications of the ACM*, *47*(3), 66-68 (2004)
15. Murphy, R.R.: A decade of rescue robots. In: *IEEE/RSJ International Conference on Intelligent Robots and Systems* (pp. 5448-5449). IEEE (2012)
16. Kristoffersson, A., Eklundh, K.S., & Loutfi, A.: Measuring the quality of interaction in mobile robotic telepresence: A pilot's perspective. *International Journal of Social Robotics* **5**(1), 89-101 (2013)
17. Paulos, E. and Canny, J.: Designing personal tele-embodiment. In: *Proceedings of the IEEE International Conference on Robotics and Automation* pp. 3173–3178, (1998).
18. Paulos, E. and Canny, J.: Social tele-embodiment: understanding presence. *Autonomous Robots*, vol. 11, no. 1, pp. 87–95 (2001)
19. Adalgeirsson, S.O., Breazeal, C.: MeBot: a robotic platform for socially embodied presence. In: *Proceedings of the 5th ACM/IEEE International Conference on Human-Robot Interaction (HRI)*, pp. 15–22, Osaka, Japan, (2010)
20. Burgard, W., Trahanias, P., Hähnel, D., Moors, M., Schulz, D., Baltzakis, H. & Argyros, A.: Tele-presence in populated exhibitions through web-operated mobile robots. *Autonomous Robots*, **15** (3), 309-316 (2003)
21. Chaudary, B., Paajala, I., Keino, E. & Pulli, P.: Tele-guidance based navigation system for the visually impaired and blind persons. *eHealth 360°* (pp. 9-16). Springer, Cham. (2017)
22. Double robotics website, <https://www.doublerobotics.com/> Last accessed on 26/05/2020
23. IEEE Spectrum article, <https://spectrum.ieee.org/automaton/robotics/humanoids/toyota-gets-back-into-humanoid-robots-with-new-thr3> Last accessed on 26/05/2020
24. Toyota website, <https://newsroom.toyota.co.jp/en/detail/19666346>, Last accessed on 26/05/2020
25. Whitney, J.P., Chen, T., Mars, J. & Hodgins, J.K.: A Hybrid Hydrostatic Transmission and Human-Safe Haptic Telepresence Robot In: *IEEE International conference on robotics and automation*, Stockholm, Sweden, pp. 690-695 (2016)
26. Bodner, J., Wykypiel, H., Wetscher, G., & Schmid, T.: First experiences with the da Vinci™ operating robot in thoracic surgery. *European Journal of Cardio-thoracic surgery* **25**(5), 844-851 (2004)
27. Quinetiq Dragon Runner, <https://www.qinetiq-na.com/products/unmanned-systems/dragon-runner>, Last accessed 26/05/2020
28. Xsens website, <https://www.xsens.com/cases/robo-sally-bomb-disposal-robot> Last accessed on 26/05/2020
29. Abe, K., Shiomi, M., Pei, Y.C., Zhang, T.Y., Ikeda, N. & Nagai, T.: ChiCaRo: tele-presence robot for interacting with babies and toddlers. *Advanced Robotics* **32** (4), 176-190 (2018)
30. Ilias, B., Shukor, S.A., Yaacob, S., Adom, A.H., & Razali, M.M.: A nurse following robot with high speed Kinect sensor. *ARPN Journal of Engineering and Applied Sciences*, *9*(12), 2454-2459 (2014)
31. Ardanuy, P., Otto, C., Head, J., Powell, N., Grant, B. & Howard, T.: Telepresence Enabling Human and Robotic Space Exploration and Discovery: Antarctic Lessons Learned, In: *Space, Long Beach California, USA*, p. 6756 (2005)
32. Kron, A., Schmidt, G., Petzold, B., Zah, M., Hinterseer, P. & Steinbach, E.: Disposal of explosive ordnances by use of a bimanual haptic telepresence system. In: *IEEE International Conference on Robotics and Automation, New Orleans, LA, USA Vol. 2*, pp. 1968-1973 (2004)
33. Talha, M., Ghalamzan, E.A.M., Takahashi, C., Kuo, J., Ingamells, W. & Stolkin, R.: Towards robotic decommissioning of legacy nuclear plant: Results of human-factors experiments with tele-robotic manipulation, and a discussion of challenges and approaches for decommissioning. In: *IEEE International Symposium on Safety, Security, and Rescue Robotics, Lausanne, Switzerland*, pp. 166-173 (2016)
34. West, C., Monk, S., Montazeri, A. and Taylor, C.J.: A vision-based positioning system with inverse dead-zone control for dual-hydraulic manipulators. In: *UKACC 12th International Conference on Control, Sheffield, UK, IEEE* (2018);
35. Tsitsimpelis, I., Taylor, C. J., Lennox, B., & Joyce, M. J.: A review of ground-based robotic systems for the characterization of nuclear environments. *Progress in Nuclear Energy*, *111*, 109-124 (2019)
36. Colgate, E., Bicchi, A., Peshkin, M. A., & Colgate, J. E.: Safety for physical human-robot interaction. In: *Springer handbook of robotics* (pp. 1335-1348) Springer (2008)
37. Kulić, D., & Croft, E.: Pre-collision safety strategies for human-robot interaction. *Autonomous Robots*, **22**(2), 149-164 (2007)
38. RIA/ANSI R15.06—1999 American National Standard for Industrial Robots and Robot Systems—Safety Requirements. American National Standards Institute. New York.
39. Hussein, M.A., Ali, A.S., Elmisery F. & Mostafa, R.: Motion Control of Robot by using Kinect Sensor, *Research Journal of Applied Sciences, Engineering and Technology* **8** (11), 1384-1388 (2014)
40. Marturi, N., Rastegarpanah, A., Takahashi, C., Adjigble, M., Stolkin, R., Zurek, S., Kopicki, M., Talha, M., Kuo, J.A., Bekiroglu, Y.: Advanced robotic manipulation for nuclear decommissioning: A pilot study on tele-operation and autonomy. In: *Proceedings of the International Conference on Robotics and Automation for Humanitarian Applications, Kerala, India*. pp. 1–8 (2016)